Physics – Uspekhi **63** (4) 388 – 394 (2020)

INSTRUMENTS AND METHODS OF INVESTIGATION PACS numbers: **07.81. + a**, 29.30 Aj, 41.85.Ar

Method of detection and spectrometry of charged particles produced in a superstrong electromagnetic field based on their transport by the magnetic field of a coaxial line

S I Moshkunov, V Yu Khomich

DOI: https://doi.org/10.3367/UFNe.2019.10.038685

Contents

Abstract. This paper presents methods of detection and spectrometry of high-energy electrons and positrons produced in the interaction of laser radiation with matter and vacuum. The methods are based on charged particle transport in the magnetic field of a hollow coaxial line through which a direct current flows. The methods make it possible to detect particles at a distance of several dozen meters from the source with retention of close to 100% collection efficiency and provide efficient detector protection from background radiation.

Keywords: positron, detector, time-of-flight magnetic spectrometer

1. Introduction

The experimental investigation of the effects occurring in strong electromagnetic fields — which is of interest in the development of quantum electronics and its applications, as well as in the verification of several predictions of quantum electrodynamics — has become possible due to achievements in the area of generating ultraintense electromagnetic radiation made in recent decades. This is largely due to advances in pico- and femtosecond lasers [1–5] and laser fusion research [6–8]. Today, by focusing the pulses of high-power laser devices, it is possible to obtain electromagnetic radiation with an intensity of $10^{20} - 10^{22}$ W cm^{-2} in laboratory conditions [5–10]. Projects are underway aimed at raising the intensity of laser radiation up to 10^{26} W cm^{-2} in the near future [11].

Even the advent of the first, relatively unsophisticated, pulsed lasers lent impetus to the appearance of theoretical papers concerned with the interaction of ultrahigh laser fields with matter and vacuum [12–20]. Most interesting among the findings of these investigations, in our view, is the prediction of the possibility of electron-positron pair production in the interaction of laser radiation with matter [15, 18, 19], vacuum [14, 15, 21–23], and free electrons [20, 24].

The last decade has seen experimental investigations of the interaction of strong electromagnetic fields of laser radiation with matter at several research centers [25–29]. The investigations showed that these experiments entail the emission of a large number of electrons, ions, and X-ray photons, these events being confined in a narrow spatio-temporal domain [5, 8]. Consequently, these experimental conditions are characterized by extremely strong background radiation. According to theoretical calculations, both in the case of electron-positron pair production in a laser field [12–24] and in the case of enhancement of beta decay under laser irradiation [30], the expected number of emission events per laser pulse is rather small ($\sim 1 - 100$). Furthermore, ultra-high-intensity laser systems have a short pulse duration and operate at a low pulse repetition rate ($\leqslant 0.1$ Hz) [8], making practically inefficient the use of sequential data processing methods employed in nuclear physics experiments with charged particle accelerators and radioactive sources.

Successful execution of the experiments under consideration calls for basically new approaches to solve the problem of detection and energy measurement of a small number of light

S I Moshkunov (*), **V Yu Khomich**
Institute for Electrophysics and Electric Power, Russian Academy of Sciences,
Dvortsovaya naberezhnaya 18, 191186 St. Petersburg, Russian Federation
E-mail: (*)serg-moshkunov@yandex.ru

Received 27 March 2019
Uspekhi Fizicheskikh Nauk **190** (4) 421 – 428 (2020)
Translated by E N Ragozin; edited by B L Derbov

charged particles, electrons and positrons, under conditions of the high-intensity corpuscular and X-ray background generated by laser-produced plasma.

The use of a nonuniform magnetic field to provide the drift (transport) of oppositely charged particles in opposite directions seems to be the most fruitful idea in the solution to this problem. In particular, Thibaud [31] came up with the method of extracting and transporting the particles to be recorded to the detector using the nonuniform magnetic field of the peripheral region of an electromagnet with a core (the trochoid method). The method permits placing the detector at a considerable distance from the source (up to ~ 40 cm) for background protection and is characterized by a high efficiency (up to $\sim 30\%$ of 4π sr) in the broad particle energy range from 0.1 to 3 MeV [31–33]. However, further improvement of the above parameters with the trochoid method, as well as other known methods [33], involves major technical difficulties, specifically, the growth of the size and weight of the electromagnet wit a core.

2. Transport of charged particles by the magnetic field of a current-carrying coaxial line

In this section, we consider a method which makes it possible to transport charged particles over a long distance (~ 10 m for electrons and positrons) with an efficiency close to 100% [34]. The method is based on the effect of charged particle drift in the magnetic field of a linear current-carrying conductor in the direction parallel to the conductor.

The motion of a charged particle in the field of an infinite linear conductor with current I was considered at length in Ref. [35]. The equation of motion of a particle with mass m, charge q, and velocity v in the cylindrical coordinate system (r, φ, z), where axis z coincides with the direction of the current, has the form (the dots above the symbols denote time derivatives)

$$\ddot{r}-r\dot{\varphi}^2+\frac{v\dot{z}}{wr}=0\,, \quad \frac{\mathrm{d}}{\mathrm{d}t}(r^2\dot{\varphi})=0\,, \quad \ddot{z}+r\dot{\varphi}^2-\frac{v\dot{r}}{wr}=0\,, \quad (1)$$

where

$$w=\frac{2\pi mv}{\mu_0 qI}\left(1-\frac{v^2}{c^2}\right)^{-1/2}$$

is a dimensionless parameter which characterizes the particle velocity, μ_0 is the magnetic constant, and c is the speed of light. The solution of Eqns (1) has the form [35]

$$t=\pm\int\frac{\mathrm{d}r}{v\sqrt{f(r)}}\,, \quad z=\pm\int\frac{\ln(r/d)\,\mathrm{d}r}{w\sqrt{f(r)}}\,,$$

$$\varphi=\pm\int\frac{b^2\,\mathrm{d}r}{vr^2\sqrt{f(r)}}\,, \qquad (2)$$

where

$$b=r_0^2\dot{\varphi}(0)\,, \quad d=r_0\exp\left[-\frac{\dot{z}(0)w}{v}\right],$$

$$f(r)=1-\left[\frac{1}{w}\ln\left(\frac{r}{d}\right)\right]^2-\left(\frac{b}{vr}\right)^2,$$

and r_0 is the value of coordinate r at the initial moment of time. It may be shown that these solutions possess the following properties [35]:

(1) $r(t)$, $\dot{\varphi}(t)$, and $\dot{z}(t)$ are periodic functions with a period T dependent on the initial conditions. Figure 1 shows two special cases of the trajectory of motion. In the general case, the particle motion is the superposition of motions along the trajectories $\varphi=\text{const}$ and $r=\text{const}$.

(2) for any initial conditions, the following inequality holds:

$$\exp(-2w)\leqslant\frac{r(t)}{r_0}\leqslant\exp(2w)\,. \qquad (3)$$

(3) irrespective of the initial condition, the motion, on average, proceeds along the z axis, positively charged particles drifting in the direction of the current and the negatively charged ones drifting in the opposite direction.

These results suggest that the particles emitted in an arbitrary direction by a point source located at distance r_0 from the axis move, on average, along the conductor and remain inside the cylindrical layer defined by inequality (3). If the detector has the shape of a ring coaxial with the conductor (see Fig. 1), the ring size taken in accordance with inequality (3), a particle emitted by the point source in any direction hits the detector irrespective of the source–detector distance, i.e., the transport efficiency of this system is equal to 100%.

For a given current, the maximum transported particle energy depends on the geometry of the system, and therefore below we consider the transport device in the form of a coaxial line. Since the field inside the coaxial line is equivalent to the field of an infinite linear conductor, all previous conclusions remain in force. Let the inner and outer radii of coaxial line conductors be R_1 and R_2, respectively. Then, from the condition $R_1\leqslant r(t)\leqslant R_2$ and inequality (3), we find that the transport efficiency is 100% for the optimal position of the point source $r_0=\sqrt{R_1R_2}$ for any particle energies E, where

$$E\leqslant mc^2\left[\sqrt{1+\left(\frac{\mu_0 qI}{8\pi mc}\ln\frac{R_1}{R_2}\right)^2}-1\right]. \qquad (4)$$

For $I=100$ kA, $R_1/R_2=20$, $q=e$, and $m=m_e$, we obtain $E=4.6$ MeV. The specified current may be obtained by discharging a capacitor through a closed coaxial line. For a characteristic time of the order of 1 ms, a closed coaxial line about 10 m long manifests itself as an inductor, and on closing the switching element, a sinusoidal current pulse is formed. If the loss in the electric circuits is ignored, the energy W_C stored in the capacitor is determined by the energy of the magnetic field inside the coaxial line W_B at the maximal current:

$$W_C=W_B=\frac{LI^2}{2}\,, \qquad (5)$$

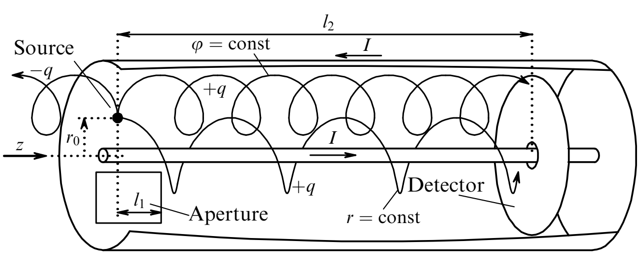

Figure 1. Charged particle transport in the magnetic field of a current-carrying coaxial line.

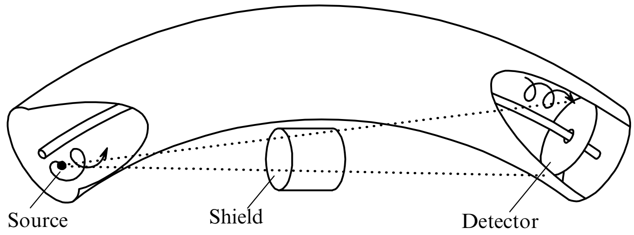

Figure 2. Detector protection from direct X-rays from the source.

where $L = (\mu_0 l)/(2\pi) \ln(R_1/R_2)$ is the inductance of the coaxial line of length l. For given values of E, R_1/R_2, and l, from expressions (4) and (5) we obtain

$$W_C = W_B = l \, \frac{16\pi(E^2 - m^2c^4)}{\mu_0 q^2 c^2 \ln(R_1/R_2)} \, .$$

For $R_1/R_2 = 20$, $q = e$ and $m = m_e$, and $E = 1.5$ MeV, we obtain $W_B/l = 330$ J m^{-1}. For a moderate energy value $W_B = 10$ kJ, we obtain $l \approx 30$ m.

To protect the detector from X- and gamma-ray radiation, the coaxial line may be given a curved shape, and a lead shield may be placed between the source and the detector (Fig. 2).

Due to the complexity of particle trajectories and significant detector remoteness, the method makes it possible to obtain a long delay between the instants of particle emission and detection. For instance, for $E = 1.5$ MeV, $l = 2$ m, and $I = 100$ kA, numerical integration of Eqns (2) yields electron flight times of 36–72 ns. This delay makes it much easier to detect particles when they are emitted simultaneously with a short intense X-ray pulse (for instance, the bremsstrahlung of a laser-produced plasma or of an accelerator beam.

3. Drift velocity of a charged particle in the magnetic field of a coaxial line

The drift velocity of a charged particle, which is equal to the ratio of its axial displacement in a radial oscillation period to the value of this period, is obtained from Eqns (2):

$$v_d = \int_{r_{min}}^{r_{max}} \frac{v \ln(r/d) \, dr}{w\sqrt{f(r)}} \left(\int_{r_{min}}^{r_{max}} \frac{dr}{\sqrt{f(r)}} \right)^{-1} , \tag{6}$$

where r_{min} and r_{max} are the roots of equation $f(r) = 0$. Depending on the direction of charged particle emission, the highest and lowest values of the drift velocity correspond to the two limiting cases, $r = \text{const}$ and $\varphi = \text{const}$, and are given by the expressions [35]

$$v_d = \frac{2vw}{\sqrt{1 + 4w^2} + 1} \, , \quad r = \text{const} \, , \tag{7}$$

$$v_d = \frac{v \, i J_1(iw)}{J_0(iw)} \, , \quad \varphi = \text{const} \, , \tag{8}$$

where $J_k(x)$ is the Bessel function of order k. For small w values, the highest-to-lowest drift velocity ratio tends to the value 2, which coincides with the result of the perturbation theory [36]. With increasing w, the highest and lowest drift velocities tend to an instantaneous velocity, and their ratio tends to unity.

4. Spectrometry of charged particles in their transport by the magnetic field of a current-carrying coaxial line

The time-of-flight method of electron spectrometry [37, 38] is based on electron transport by the magnetic field of a hollow current-carrying coaxial line. Under the action of the magnetic field, the electrons emitted by the source drift (are transported) to a ring-shaped detector located at the coaxial line end opposite to the source. When the flight base l is much longer than the electron orbit diameter, the flight time τ is

$$\tau = \frac{l}{v_d} \, . \tag{9}$$

Since the drift velocity v_d of a charged particle depends strongly on its energy E even for relativistic velocities, measuring its flight time τ permits the particle energy to be determined from expressions (9) and (6). Measuring the flight time distribution for a group of particles makes it possible to determine their energy spectrum. It is significant that the drift velocity in the field of this configuration is independent of the distance of the point of charged particle emission from the axis of the coaxial line and is defined only by the current I, which is easily monitored to the requisite accuracy. Adherence to condition (4) for the highest energy of the spectrum under measurement provides charged particle transport to the detector from the complete solid angle. Consequently, the spectrometer efficiency may be as high as 100% of 4π sr.

The main limitation on the accuracy of charged particle energy with the above method is the dependence of the drift velocity on the direction of the particle emission by the source. In this case, electrons with energies in some interval $E_1 - E_2$ may have the same drift velocity. The energy resolution may then be written as

$$R = \frac{2(E_1 - E_2)}{E_1 + E_2} \, .$$

Figure 3 depicts the dependence of the resolution on parameter w, which was obtained from expressions (7) and

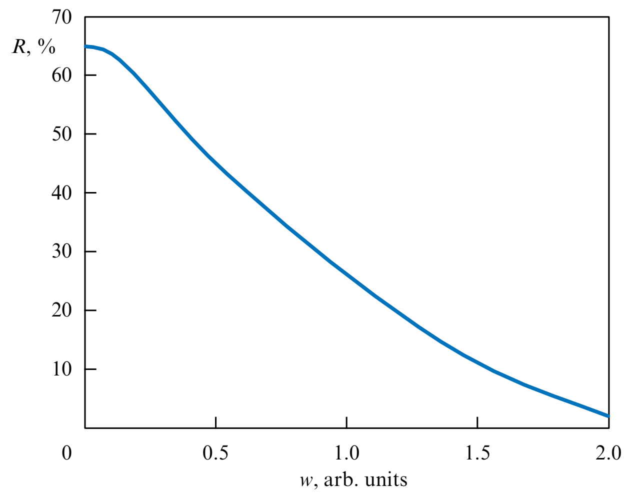

Figure 3. Resolution (R) of a spectrometer without an aperture as a function of parameter w.

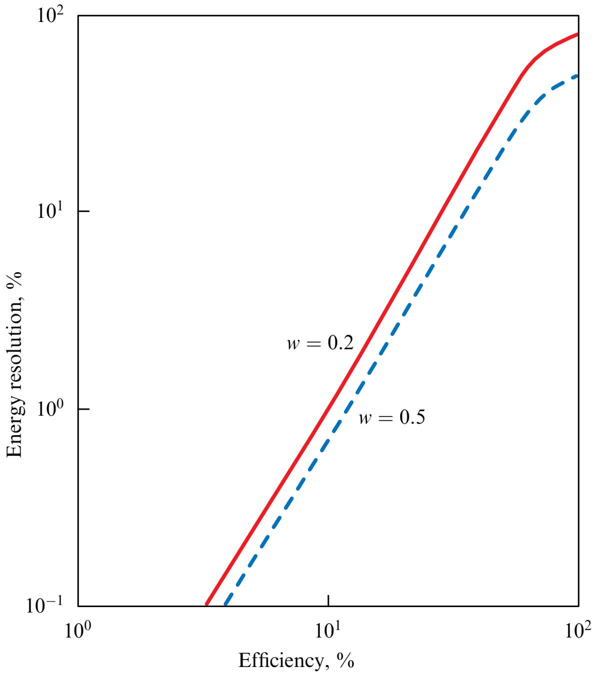

Figure 4. Resolution of a spectrometer with an aperture versus its efficiency for two values of parameter w.

(8). It is noteworthy that particle trajectories with a greater variation of coordinate r (expression (3)) correspond to higher w values, which requires the use of a coaxial line with the corresponding outer-to-inner conductor radius ratio. The range $R_1/R_2 = 10-100$ may be considered practically realizable, whence it follows that $R = 22-66\%$.

We consider possible ways of improving the resolution by limiting the solid angle with an aperture. The results of numerical integration of expression (6) are plotted in Fig. 4. One can see that the resolution improves rapidly as the solid angle (efficiency) is limited. Specifically, for a efficiency of 10% of 4π sr, the resolution is 0.8–1%, sufficient for many applications, including electron spectroscopy.

Next, we consider one of the possible versions of aperture positioning, shown in Fig. 1. Electrons with a rather high azimuthal velocity collide with the aperture stop and are absorbed, which results in improvement of the energy resolution. For a given energy resolution, the aperture length is given by the expression

$$l_1 = \frac{\pi v r_0 (1 + R)}{2a\sqrt{R}} \,.$$

Figure 5 shows the spectrometer efficiency and resolution in the 10–100 keV electron energy range, which were calculated for the following parameter values: $I = 100$ kA, axis-source distance $r_0 = 1$ cm, aperture length $l_1 = 5$ cm, and source–detector distance $l = 2$ m (see Fig. 1). A spectrometer with these parameters holds considerable promise for the investigation of electron emission from laser-produced plasmas. With retention of the energy resolution of at least 10% efficiency the energy measurement range, its efficiency is higher than 20%. This is two orders of magnitude greater than in commonly employed magnetic spectrometers with a uniform field.

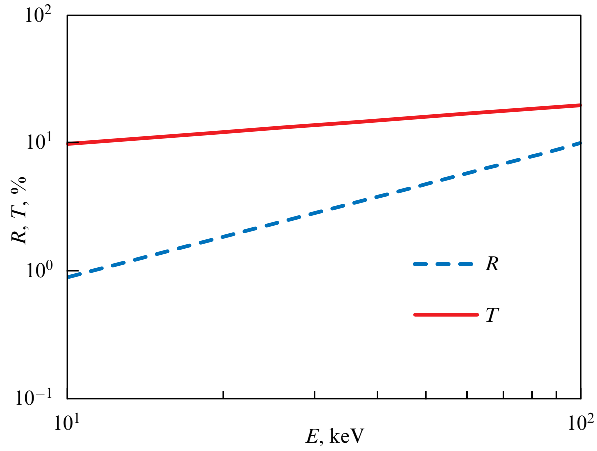

Figure 5. Dependence of spectrometer efficiency T and resolution R on the electron energy calculated for $I = 100$ kA, $r_0 = 1$ cm, $l_1 = 5$ cm, and $l = 2$ m.

5. Experimental facility

Based on the above method, an experimental facility was made for investigating the particle emission from laser-produced plasmas (Fig. 6) [39, 40]. A curved 2-m-long coaxial line was used to transport particles to the detector.

In view of the low repetition rate of laser pulses, a pulsed current generator with a duration much longer than the characteristic transport time of the particles under study is well suited to these experiments. The electric generator circuit is presented in Fig. 7. Use was made of a circuit with a total discharge of the storage capacitor. On triggering the discharge, a current appears in the coaxial line in the form of a slowly decaying sinusoid with a period of 246 µs (Figs 8 and 9). For the highest capacitor charging voltage of 5000 V (energy: 15 kJ), the current amplitude was about 96 kA for the first positive peak and 87 kA for the first negative one. A mutual temporal arrangement of the current pulse and the laser pulse required for the operation of the system was realized by timing the actuation of the laser system to the maximum or minimum of the current curve in the coaxial line for the operation with positively (see Fig. 8)

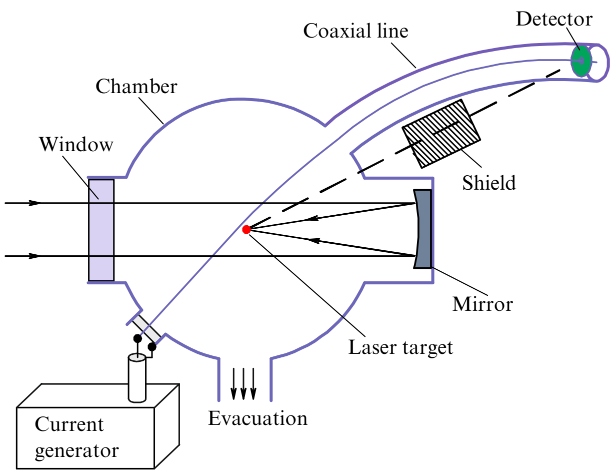

Figure 6. Facility for the investigation of fast charged particle production in strong laser fields.

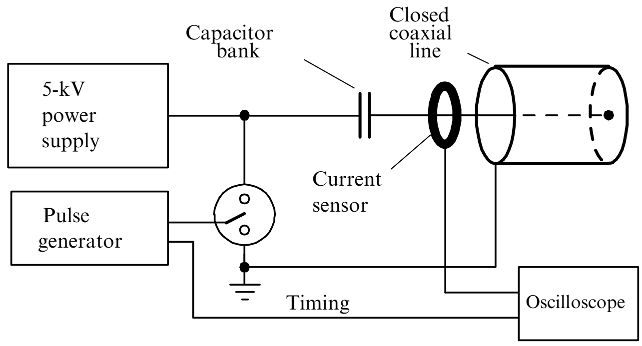

Figure 7. Circuit of a pulsed current generator.

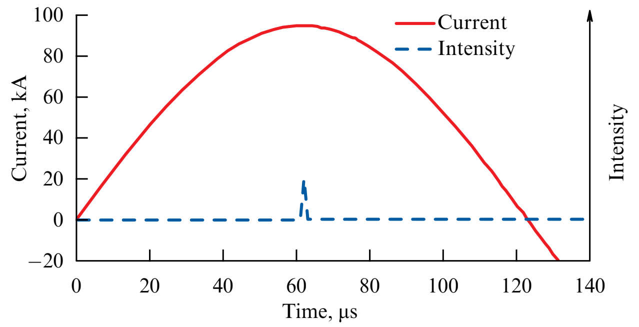

Figure 8. Timing of the current curve (solid line) and the laser pulse (dashed line) for transporting positively charged particles.

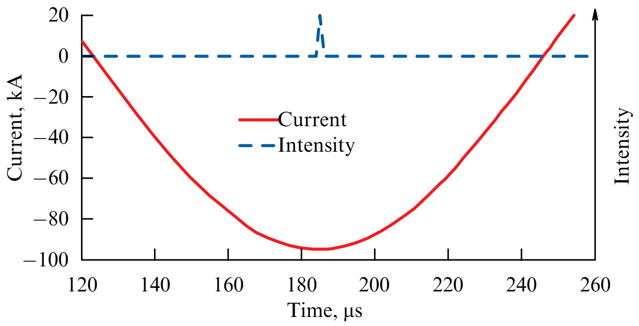

Figure 9. Timing of the current curve (solid line) and the laser pulse (dashed line) for transporting negatively charged particles.

or negatively (see Fig. 9) charged particles, respectively [41, 42].

To detect electrons and positrons with energies above 30 keV emitted by the laser-produced plasma, a scintillation detector was developed [42]. A detector of this type was chosen in order to combine a relatively large aperture (about 100 mm), a high efficiency, a high temporal resolution, and immunity of the sensitive detector region to electromagnetic interference and a strong magnetic field. The detector is shown in Fig. 10. The detector consists of a polystyrene ring-shaped scintillator 90 mm in diameter, which is positioned between the conductors of the coaxial line and spans almost all of its cross section. The scintillator is 4 mm thick, which provides total absorption of electrons and positrons with energies of up to 1 MeV. An optical waveguide extracts the light of a scintillation flash beyond the coaxial line, as shown in Fig. 10, which is recorded with two photomultipliers (FEU-184-T) with an aperture of 52 mm to maximize the

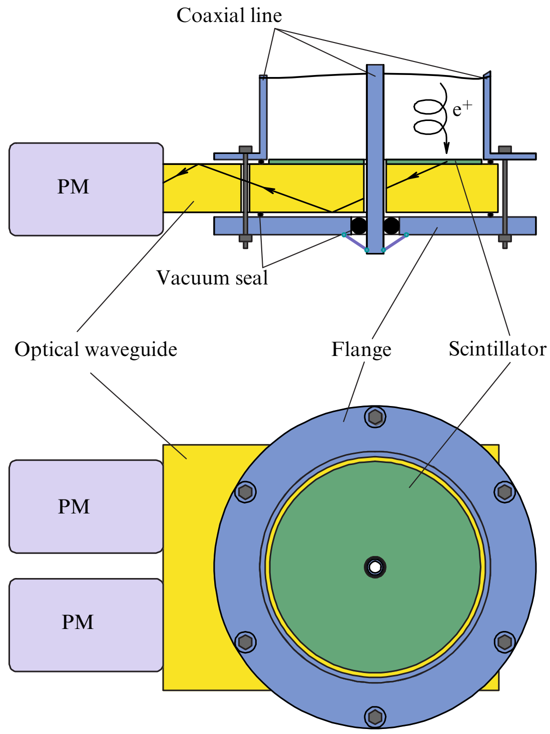

Figure 10. Scintillation detector of charged particles.

coverage of the optical waveguide end and to lower the probability of spurious signals.

The six tightening bolts evenly distributed over the circumference provide the necessary path for the flow of a high current and at the same time the rapid decay of a magnetic field beyond the coaxial line, thereby creating normal conditions for photo multiplier (PM) operation.

6. Experiment with a radioactive electron source

To estimate the efficiency of detection of high-energy electrons with the proposed method, experiments were carried out with a certified radioactive electron source based on the Cs^{137} isotope. A source with a planar geometry, in which the isotope was placed between two polyethylene films fixed in a barrel 29 mm in diameter, was mounted close to the inner conductor of the coaxial line in the plane passing through its axis. This orientation minimizes the possibility of repeated collisions of the outgoing electrons with the structural elements of the radioactive source.

The method of measuring the electron detection efficiency involved measurements of the average frequency of electron detection events in those time intervals when the current in the coaxial line had the sign and value required for transporting electrons to the detector.

The block diagram of the data collection system is shown in Fig. 11. The signals from the two PMs are initially delivered to pulse discriminators and then to a coincidence circuit. The pulses from the coincidence circuit arrive at the input of a gated pulse counter. A 60 μs-long gating pulse is applied to the counter with a 61.5-μs delay relative to the pulse triggering the discharge of the pulse generator. As a result, the middle of the gating pulse coincides in time with the peak of the coaxial line current.

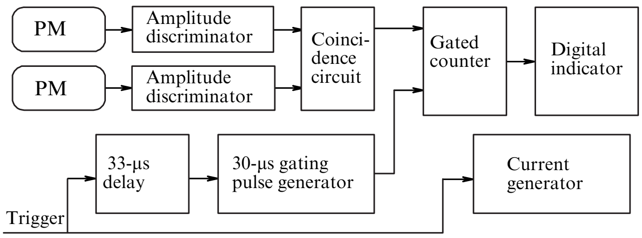

Figure 11. System of PM signal collection and processing.

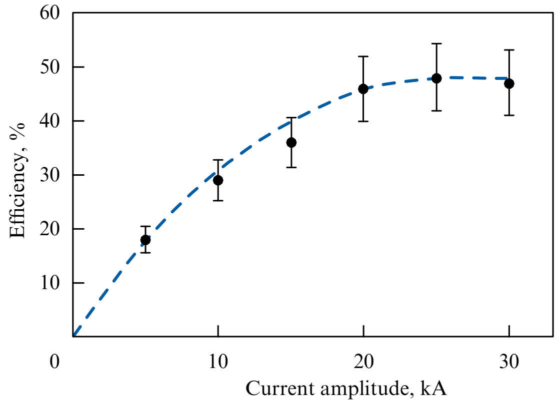

Figure 12. Efficiency of electron detection system versus the current amplitude in the coaxial line.

The efficiency of electron detection was determined from the expression

$$T = \frac{N}{n\,\Delta t A_\beta (1-k)}\,,$$

where N is the total number of pulses recorded by the counter, n is the number of current generator triggerings in a given series of measurements, Δt is the gating pulse duration, A_β is the certified beta-activity of the radioactive source, and k (4%) is the proportion of electrons absorbed by the polyethylene film of the holder calculated based on the known electron distribution function for Cs^{137}.

Figure 12 shows the efficiency measured as a function of the current amplitude in the coaxial line. The peak efficiency of 48 ± 6% of 4π sr was measured for a current of 25 kA.

To evaluate the efficiency of electron transfer to the detector, the source, alternately by each of its flat sides, was attached closely to the scintillator. The detector efficiency was measured from the expression

$$\Omega = \frac{f_1 + f_2}{A_\beta (1-k)} = 0.52\,,$$

where f_1, f_2 are the coincidence frequencies for each of the source sides. From this estimate, it follows that the measured efficiency of the spectrometer as a whole (48% of 4π sr) is determined primarily by the detector efficiency, while the transport efficiency amounts to about 90% of 4π sr.

7. Results of experiments with laser-produced plasma

The experimental facility described in Section 5 was employed to perform experiments with laser-produced plasma. The plasma was produced by TEA CO_2 laser radiation with a pulse duration of 50 ns, which was focused with an $f = 30$ cm lens (see Fig. 6) on a metal target in the form of a 0.2–0.4-mm wire. The on-target radiation intensity was $\sim 10^{13}$ W cm^{-2}. For a detector, use was made of a charge collector in the form of a flat stainless steel disk, which spanned almost the entire cross section of the coaxial line. Figure 13 shows typical oscillograms of the collector current (a–c) and the laser pulse (d). The curve in Fig. 13a was obtained in the absence of current through the coaxial line. Here, the positive peak with practically zero delay relative to the laser pulse is due to the photoeffect at the collector, while the tail arises from the arrival of plasma particles at the collector as a result of scattering from the chamber walls. The oscilloscope trace in Fig. 13b was obtained for a current of 32 kA directed, in the inner conductor, from the detector to the source. The collector signal is a negative pulse more than 20-fold greater in amplitude than the curve in Fig. 13a, with the characteristic delay relative to the laser pulse. It is pertinent to note that the time delay increases linearly with the current in the coaxial line.

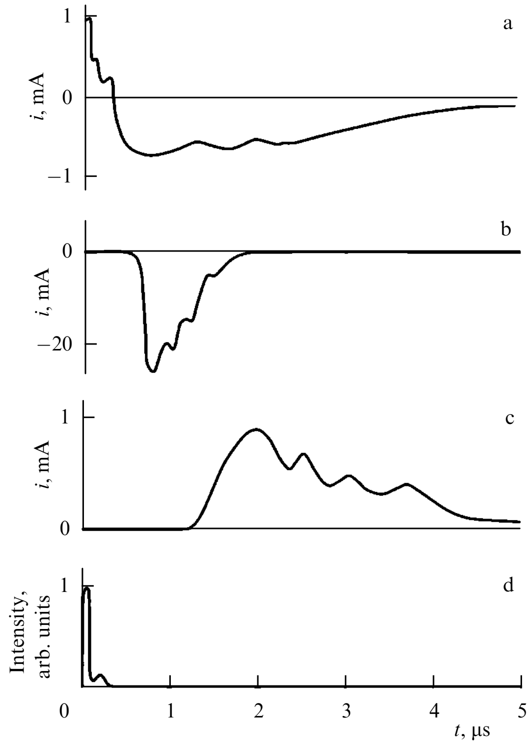

Figure 13. Oscillograms of the collector current (a–c) and the laser pulse (d) recorded for $r_0 = 1$ cm, $l = 2$ m, $I = 0$ (a), $I = -32$ kA (b), and $I = +32$ kA (c).

For the opposite current direction in the coaxial line, the collector signal has positive polarity (Fig. 13c) and is caused by the arrival of expanding plasma ions at the collector. In this case, the delay is about 1 μs and is almost independent of the current strength.

The electron spectra were measured using the time-of-flight method described in Section 4. A typical oscillogram of collector current and the laser-plasma emitted electron spectrum calculated from this trace are given in Figs 14 and 15, respectively. The characteristic form of the curves testifies to the presence of suprathermal electrons in the spectrum.

Attempts to detect positrons at this facility did not meet with success. Based on the measured high sensitivity of the

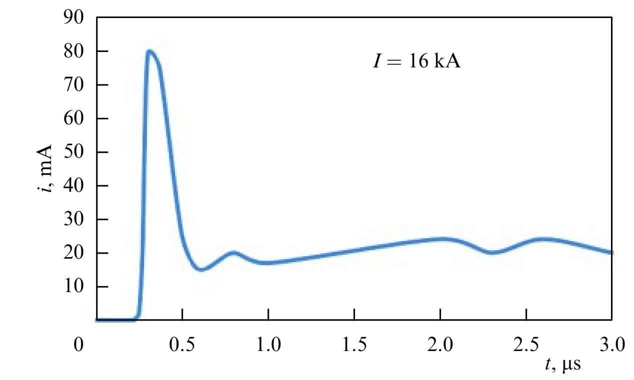

Figure 14. Typical collector oscillogram i for $I = 16$ kA, $r_0 = 1$ cm, $l_1 = 1$ cm, and $l = 2$ m. The intensity of focused laser radiation $\approx 2 \times 10^{13}$ W cm^{-2}, $\lambda = 10.6$ µm.

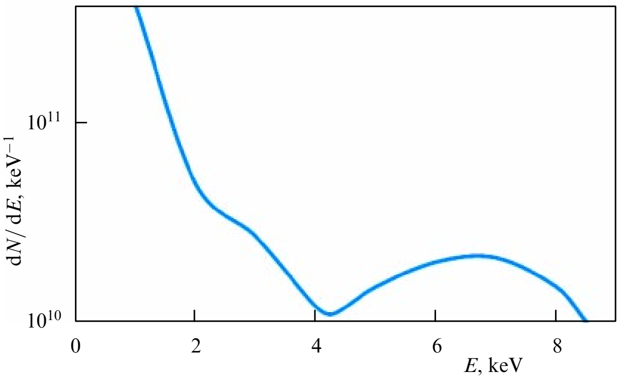

Figure 15. Energy spectrum of the electrons emitted by a laser-produced plasma, which was calculated by processing the oscilloscope trace of Fig. 14.

detection system, we concluded that electron-positron pairs are not produced at intensities of $\leqslant 10^{13}$ W cm^{-2}.

8. Conclusions

Our paper presents the results of theoretical and experimental investigations involving the development and implementation of a new class of selective high-efficiency systems for the detection and spectrometry of charged particles, which rely on the particle transport in the magnetic field of a coaxial line. We have shown the feasibility of attaining a close to 100% throughput in the broad particle energy range of 0.1–3 MeV for a considerable source–detector distance.

The design parameters of the detector and pulsed magnetic field generator were optimized for the efficient detection of charged particles generated in superstrong electromagnetic fields. By way of simulations, it was possible to determine the relation between the spectrometer resolution and efficiency upon introducing an aperture to limit the solid angle of particle emission.

The electron and positron detection system designed on the basis of this method was experimentally investigated. The system combines a high efficiency (50%) in a broad energy range and a high degree of immunity to background source radiation. Experiments were carried out in the time-of-flight spectrometry of the high-energy electrons emitted by laser-produced plasma. The feasibility of extracting and measuring the spectrum of suprathermal electrons emitted by the laser-produced plasma was experimentally demonstrated.

Acknowledgements

The authors express their appreciation to E A Shershunova for his support of the work and fruitful discussions.

References

1. Voronin A A et al. *Opt. Commun.* **291** 299 (2013)
2. Khazanov E A, Sergeev A M *Phys. Usp.* **51** 969 (2008); *Usp. Fiz. Nauk* **178** 1006 (2008)
3. Xu L et al. *Opt. Lett.* **38** 4837 (2013)
4. Pittman M et al. *Appl. Phys. B* **74** 529 (2002)
5. Korzhimanov A V et al. *Phys. Usp.* **54** 9 (2011); *Usp. Fiz. Nauk* **181** 9 (2011)
6. Taylor D et al. *High Energy Density Phys.* **9** 363 (2013)
7. Key M H et al. *Phys. Plasmas* **5** 1966 (1998)
8. Chen H et al. *Phys. Plasmas* **24** 033112 (2017)
9. Bahk S-W et al. *Opt. Lett.* **29** 2837 (2004)
10. Yanovsky V et al. *Opt. Express* **16** 2109 (2008)
11. Mourou G A et al. *Opt. Commun.* **285** 720 (2012)
12. Keldysh L V *Sov. Phys. JETP* **20** 1307 (1965); *Zh. Eksp. Teor. Fiz.* **47** 1945 (1964)
13. Gol'dman I I *Sov. Phys. JETP* **19** 954 (1964); *Zh. Eksp. Teor. Fiz.* **46** 1412 (1964)
14. Nikishov A I *Tr. Fiz. Inst. Akad. Nauk SSSR* **111** 152 (1979)
15. Bunkin F V, Tugov I I *Sov. Phys. Dokl.* **14** 678 (1970); *Dokl. Akad. Nauk SSSR* **187** 541 (1969)
16. Bunkin F V, Kazakov A E *Sov. Phys. Dokl.* **15** 758 (1971); *Dokl. Akad. Nauk SSSR* **193** 1274 (1970)
17. Bunkin F V, Kazakov A E, Fedorov M V *Sov. Phys. Usp.* **15** 416 (1973); *Usp. Fiz. Nauk* **107** 559 (1972)
18. Shearer J W et al. *Phys. Rev. A* **8** 1582 (1973)
19. Hora H *Optoelectronics* **5** 491 (1975)
20. Erber T *Rev. Mod. Phys.* **38** 626 (1966)
21. Bulanov S S et al. *JETP* **102** 9 (2006); *Zh. Eksp. Teor. Fiz.* **129** 14 (2006)
22. Popov V S *JETP Lett.* **74** 133 (2001); *Pis'ma Zh. Eksp. Teor. Fiz.* **74** 151 (2001)
23. Narozhny N B et al. *JETP Lett.* **80** 382 (2004); *Pis'ma Zh. Eksp. Teor. Fiz.* **80** 434 (2004)
24. Nikishov A I, Ritus V I *Sov. Phys. Usp.* **13** 303 (1970); *Usp. Fiz. Nauk* **100** 724 (1970)
25. Rose S J *High Energy Density Phys.* **9** 480 (2013)
26. Chen H et al. *New J. Phys.* **15** 065010 (2013)
27. Belyaev V S et al. *Phys. Usp.* **51** 793 (2008); *Usp. Fiz. Nauk* **178** 823 (2008)
28. Chen H et al. *Phys. Rev. Lett.* **102** 105001 (2009)
29. Chen H et al. *High Energy Density Phys.* **7** 225 (2011)
30. Becker W et al. *Phys. Rev. Lett.* **47** 1262 (1981)
31. Thibaud J *Phys. Rev.* **45** 781 (1934); Translated into Russian: *Usp. Fiz. Nauk* **14** 833 (1934)
32. Bochev B et al. *Prib. Tekh. Eksp.* (5) 247 (1971)
33. Stolyarova E L *Prikladnaya Spektrometriya Ioniziruyushchikh Izluchenii* (Applied Spectrometry of Ionizing Radiations) (Moscow: Atomizdat, 1964)
34. Apollonov V V, Moshkunov S I, Prokhorov A M *Sov. Tech. Phys. Lett.* **11** 321 (1985); *Pis'ma Zh. Tekh. Fiz.* **11** 773 (1985)
35. Malmfors K G *Arkiv Fys.* **13** 237 (1958)
36. Alfvén H *Arkiv Mat. Astr. Fys. A* **27** (22) 1 (1940)
37. Moshkunov S I et al. *Pis'ma Zh. Tekh. Fiz.* **16** (19) 47 (1990)
38. Moshkunov S I, Sisakyan I N, Khomich V Yu "Sposob opredeleniya spektra zaryazhennykh chastits" ("Method for determining the spectrum of charged particles"), Author's Certificate No. 1568750 (1988)
39. Apollonov V V et al. *Sov. J. Quantum Electron.* **16** 418 (1986); *Kvantovaya Elektron.* **13** 643 (1986)
40. Moshkunov S I, Sisakyan I N, Khomich V Yu "Ustroistvo dlya registratsii zaryazhennykh chastits" ("Device for detection of charged particles"), Author's Certificate No. 1602211 (1988)
41. Apollonov V V et al. *Proc. SPIE* **0664** 243 (1986)
42. Apollonov V V et al. *Pis'ma Zh. Tekh. Fiz.* **13** 1363 (1987)